Original Article

JCBFM

Journal of Cerebral Blood Flow & Metabolism
2022, Vol. 42(1) 162–174

DOI: 10.1177/0271678X21033362
journals.sagepub.com/home/jcbfm
SAGE

Arachnoid membrane as a source of sphingosine-1-phosphate that regulates mouse middle cerebral artery tone

Francesc Jiménez-Altayó[1], Julia Marzi[2,3,4], María Galan[5], Ana Paula Dantas[6], Marisa Ortega[7,8], Santiago Rojas[7], Gustavo Egea[9], Katja Schenke-Layland[2,3,4,10], Elena Jiménez-Xarrié[11] and Anna M Planas[12]

Abstract

Growing evidence indicates that perivascular tissue is critical to modulate vessel function. We hypothesized that the arachnoid membrane surrounding middle cerebral artery (MCA) regulates its function via sphingosine-1-phosphate (S1P)-induced vasoconstriction. The MCA from 3- to 9-month-old male and female wild-type (Oncine France 1 and C57BL/6) mice and sphingosine kinase 2 knockout (SphK2-/-) mice in the C57BL/6 background was mounted in pressure myographs with and without arachnoid membrane. Raman microspectroscopy and imaging were used for in situ detection of S1P. The presence of arachnoid tissue was associated with reduced external and lumen MCA diameters, and with an increase in basal tone regardless of sex and strain background. Strong S1P-positive signals were detected in the arachnoid surrounding the MCA wall in both mice models, as well as in a human post-mortem specimen. Selective S1P receptor 3 antagonist TY 52156 markedly reduced both MCA vasoconstriction induced by exogenous S1P and arachnoid-dependent basal tone increase. Compared to 3-month-old mice, the arachnoid-mediated contractile influence persisted in 9-month-old mice despite a decline in arachnoid S1P deposits. Genetic deletion of SphK2 decreased arachnoid S1P content and vasoconstriction. This is the first experimental evidence that arachnoid membrane regulates the MCA tone mediated by S1P.

Keywords

Arachnoid membrane, cerebral artery function, cerebral blood flow, myogenic tone, sphingosine-1-phosphate

Received 12 April 2021; Revised 27 May 2021; Accepted 25 June 2021

[1]Departament de Farmacologia, de Terapèutica i de Toxicologia, Institut de Neurociències, Facultat de Medicina, Universitat Autònoma de Barcelona, Bellaterra, Spain
[2]Department of Biomedical Engineering, Eberhard Karls University Tübingen, Tübingen, Germany
[3]NMI Natural and Medical Sciences Institute at the University of Tübingen, Reutlingen, Germany
[4]Cluster of Excellence iFIT (EXC 2180) "Image-Guided and Functionally Instructed Tumor Therapies", Eberhard Karls University of Tübingen, Tübingen, Germany
[5]Institut de Recerca de l'Hospital de la Santa Creu i Sant Pau, IIB Sant Pau, Barcelona, Spain
[6]Institut Clínic Del Tòrax, Institut D'Investigacions Biomèdiques August Pi i Sunyer (IDIBAPS), Barcelona, Spain
[7]Unit of Human Anatomy and Embriology, Department of Morphological Sciences, Faculty of Medicine, Universitat Autònoma de Barcelona, Cerdanyola del Vallès, Spain
[8]Institute of Legal Medicine and Forensic Sciences of Catalonia, Hospitalet de Llobregat, Catalonia, Spain
[9]Department of Biomedical Sciences, University of Barcelona School of Medicine and Health Sciences, Barcelona, Spain; IDIBAPS-University of Barcelona, Barcelona, Spain
[10]Department of Medicine/Cardiology, Cardiovascular Research Laboratories, David Geffen School of Medicine at UCLA, Los Angeles, CA, USA
[11]Stroke Unit, Department of Neurology, Hospital de la Santa Creu i Sant Pau (IIB-Sant Pau), Barcelona, Spain
[12]Department of Brain Ischemia and Neurodegeneration, Institut d'Investigacions Biomèdiques de Barcelona (IIBB), Consejo Superior de Investigaciones Científicas (CSIC), Barcelona, Spain; Area of Neurosciences, IDIBAPS, Barcelona, Spain

Corresponding author:
Francesc Jiménez-Altayó, Departament de Farmacologia, de Terapèutica i de Toxicologia, Institut de Neurociències, Facultat de Medicina, Av. de Can Domènech, 737, Universitat Autònoma de Barcelona, 08193 Bellaterra (Cerdanyola del Vallès), Spain.
Email: francesc.jimenez@uab.cat

Introduction

Cerebral vessels that run on the pia matter at the brain surface are surrounded by cerebrospinal fluid (CSF) that is contained within the subarachnoid space providing mechanical and immunological protection to the brain. The arachnoid mater is a fine layer located between the dura matter and the subarachnoid space that permits communication between the CSF and cerebral vessels to fine-tune crucial brain physiological responses such as supply nutrients and remove waste products.[1,2] CSF removes waste products of brain metabolism and it mediates intracerebral transport of nutrients and neuroactive substances.[3] Therefore, cerebral vessels are not only exposed to intrinsic vascular regulatory mechanisms, but also to the influence of exogenous factors such as the subarachnoid space milieu.

Sphingosine-1-phosphate (S1P) is a pleiotropic bioactive lysophospholipid generated from sphingosine phosphorylation by sphingosine kinase (SphK) 1 and 2 that acts both as an extracellular ligand and intracellular second messenger.[4] S1P is abundant in plasma where it is mainly released by erythrocytes and to a lower extent endothelial cells and platelets. However, many cells generate S1P, which is released into the extracellular environment through various membrane transporters including major facilitator superfamily domain-containing proteins Mfsd2b and Mfsd2a, spinster homolog 2 (SPNS2), and ATP-binding cassette transporters (ABCTs).[5,6] In the extracellular milieu, S1P signals in an autocrine or paracrine manner via plasma membrane G protein-coupled S1P receptors ($S1P_{1-5}R$), which participate in several essential biological responses such as vascular development and lymphocyte trafficking.[7] S1P activity ends through inactivation by ubiquitously expressed enzymes, S1P phosphatase and S1P lyase. The latter is expressed in the murine arachnoid membrane, which suggests that arachnoid S1P signaling may have so far unidentified physiological functions in this tissue.[8]

In the vasculature, S1P signaling plays important roles in the regulation of vascular development and permeability, immune cell trafficking and blood flow.[9] S1P induces Rho kinase-mediated vasoconstriction and participates in the myogenic response in vascular smooth muscle cells (VSMCs), while endothelial S1P leads to vasodilation through eNOS activation.[10] $S1P_{1-3}R$ are broadly expressed in the cardiovascular system. In the brain, S1P mediates rat and mouse basilar artery constriction mostly through $S1P_3R$ signaling.[11,12] On the other hand, SphK seems crucial for regulating S1P-dependent vasoactive actions. SphK1 activity controls myogenic responses in resistance arteries[13–16] and it has a major role in modulating vasoconstriction in rat[17] and rabbit[18] cerebral arteries. Besides, SphK2 activity protects against ischemic stroke[19] and contributes to cerebral preconditioning.[20–22] Nevertheless, the contribution of SphK2 to vasoresponsiveness is not well understood, particularly in the cerebral vasculature.

In the present study, we hypothesize that the arachnoid membrane actively participates in middle cerebral artery (MCA) responsiveness through S1P signaling. Our results demonstrate that arachnoid tissue establishes a functional crosstalk with the MCA increasing its basal tone. We show that arachnoid membrane is a reservoir of S1P in the mouse and human MCA, and we provide evidence that S1P is the mediator responsible for the arachnoid-induced vasoconstriction. Importantly, this regulatory mechanism persists during aging despite a decline in arachnoid S1P deposits. Finally, we report that SphK2 activity significantly contributes to the arachnoid-dependent S1P response.

Materials and methods

Animals

Three to 4-month-old male and female Oncine France 1 (OF1) non-consanguineous mice were obtained from Charles River (Sant Cugat del Vallès, Spain), and 3- to 4-month-old and 8- to 9-month-old male and female $SphK2^{-/-}$ mice in the C57BL/6 background and wild-type C57BL/6 mice were purchased from Jackson Laboratories (Charles River, Lyon, France). Mice were housed under controlled environmental conditions of temperature and humidity, a 12:12-h light-dark cycle, and provided with free access to food and water. Experiments were carried out following Spanish laws (Real Decreto 53/2013) and European Directives. Experiments were approved by the Ethics Committee of the *Universitat Autònoma de Barcelona* (approval code: FJA-eut/01) and the local regulatory bodies of *Generalitat de Catalunya*. Animal studies are reported following the ARRIVE guidelines.

Human subject

The MCA (M1 segment) was obtained at autopsy from a male subject (36-year-old, Caucasian), who died suddenly. Postmortem examination of the subject showed the rupture of a type A aortic aneurysm with no alterations of brain vascularization or signs of brain injury. The cadaver was less than 24 h postmortem. The human investigation committee of the *Institut de Medicina Legal i Ciències Forenses de Catalunya* approved the human study (approval code: PR 368/17).

Tissue preparation

The M1 segment of the mouse and human MCA was gently dissected, to retain and keep arachnoid tissue as

intact as possible, and kept in cold Krebs-Henseleit solution (KHS; composition in mM: NaCl 112.0; KCl 4.7; $CaCl_2$ 2.5; KH_2PO_4 1.1; $MgSO_4$ 1.2; $NaHCO_3$ 25.0 and glucose 11.1) gassed with 95 % O_2 and 5 % CO_2. MCA from mice were immediately used for pressure myography studies. In addition, both mice and human MCA segments were used for evaluation of Raman microspectroscopy and imaging and were placed in KHS containing 30 % sucrose overnight and transferred to a cryomold (Bayer Química Farmacéutica, Barcelona, Spain) containing Tissue Tek OCT embedding medium (Sakura Finetek Europe, Zoeterwoude, The Netherlands) for 15 min. Afterwards, arteries were frozen in liquid nitrogen for storage at −70 °C until Raman imaging evaluation. Additional segments of the mouse MCAs were used for immunofluorescence and were processed as described.[23]

Pressure myography

Vascular function was studied in a pressure myograph (model 114 P; Danish Myo Technology, Aarhus, Denmark) following the protocol described[24,25] with few modifications. Briefly, the MCA was placed on two glass microcannulas and carefully adjusted so that the vessel walls were parallel without stretching. A region of the artery was gently cleaned of arachnoid tissue, whereas this tissue was intentionally left intact in a contiguous region (Figure 1(a) and Supplementary Video). Afterwards, the artery was left to equilibrate for 30 min at 60 mmHg in gassed KHS (37 °C). The tissue was contracted with 100 mM KCl to assess viability. After washing and a 30 min resting time, constricted tone was induced with the stable thromboxane A2 mimetic 9,11-dideoxy-9α, 11α -methano-epoxy prostaglandin F2α (U46619; 1 nM–1 μM; EMD Millipore, Billerica, MA, USA), before adding the endothelial-dependent relaxation PAR2 agonist serine–leucine–isoleucine–glycine–arginine–leucine–NH2 (SLIGRL; 20 μM; Auspep, Tullamarine, Victoria, Australia). Afterwards, an intraluminal pressure-diameter curve (3–120 mmHg) was obtained in gassed KHS and internal and external diameters were measured for 3 min at each intraluminal pressure. After testing up to a maximum of 4 curves, the arteries were left to equilibrate for 30 min at 60 mmHg in gassed, calcium-free KHS (37 °C, 0 Ca^{2+}: omitting calcium and adding 10 mM ethylene glycol tetraacetic acid; Sigma-Aldrich, St. Louis, MO), and an intraluminal pressure-diameter curve (3–120 mmHg) was obtained in passive conditions. Myogenic parameters were studied as described.[26]

In a separate set of experiments, intraluminal pressure-diameter curves and S1P (Sigma-Aldrich, St. Louis, MO, #73914) (1 nM–1 μM) contractions were studied in the absence or presence of the $S1P_3R$ antagonist TY 52156 (4 μM; Tocris Bioscience, Bristol, United Kingdom, #5328). The concentration of TY 52156 was selected based on previous studies.[27] In addition, intraluminal pressure-diameter curves were studied in the absence or presence of the non-specific ABCA1 membrane transporter inhibitor glibenclamide (300 μM).[28] All drugs were added 30 min before starting the experiment.

Raman microspectroscopy and imaging

Frozen transverse MCA non-fixed sections (10 μm-thick) were used for Raman imaging, which was performed with a customized WiTec alpha 300 R Raman microscope (WiTec GmbH, Ulm, Germany), as described (Zbinden et al., 2020).[29] Spectral analysis was performed with the Witec Project FIVE 5.2 software (WiTec GmbH). Data sets underwent cosmic ray removal, baseline correction and normalization (area to 1) before true component analysis (TCA), as described.[30,31] Briefly, TCA is a non-negative matrix factorization based algorithm that allows to elaborate spectral signatures within the dataset and creates intensity distribution heatmaps for each identified spectral component. The S1P reference spectrum was applied to identify endogenous S1P; nuclei and elastic fiber signatures were added as contrast to the S1P signal. Characteristic peaks for each structure and their molecular assignments are shown in Supplementary Table 1. For quantitative analysis, mean gray value intensities of the Raman intensity distribution heatmaps were calculated for each component and sample in ImageJ (National Institutes of Health).

Immunofluorescence

Frozen transverse sections (14 μm-thick) previously fixed in 4% paraformaldehyde were incubated for 1 h with anti-ER-TR7 (1:50; Santa Cruz Biotechnology, Dallas, TX, #sc73355) or anti-βIII-tubulin antibody (1:50; BioLegend, San Diego, CA, #MMS-435P) primary antibodies in a humidified chamber at 37 °C. After several washes, sections were incubated with a chicken anti-rat or donkey anti-mouse IgG secondary antibodies conjugated, respectively, to Alexa Fluor® 647 (1:200; Thermo Fisher scientific, Waltham, Massachusetts, USA, #A21472) and Alexa Fluor® 546 (1:200; Thermo Fisher scientific, #A10036) in a humidified chamber at 37 °C. Sections were treated for immunofluorescence staining as described.[25] The specificity of the immunostaining was verified by exclusion of the primary antibody. Images were captured using a Leica TCS SP5 confocal microscope (Leica Biosystems, Wetzlar, Germany).

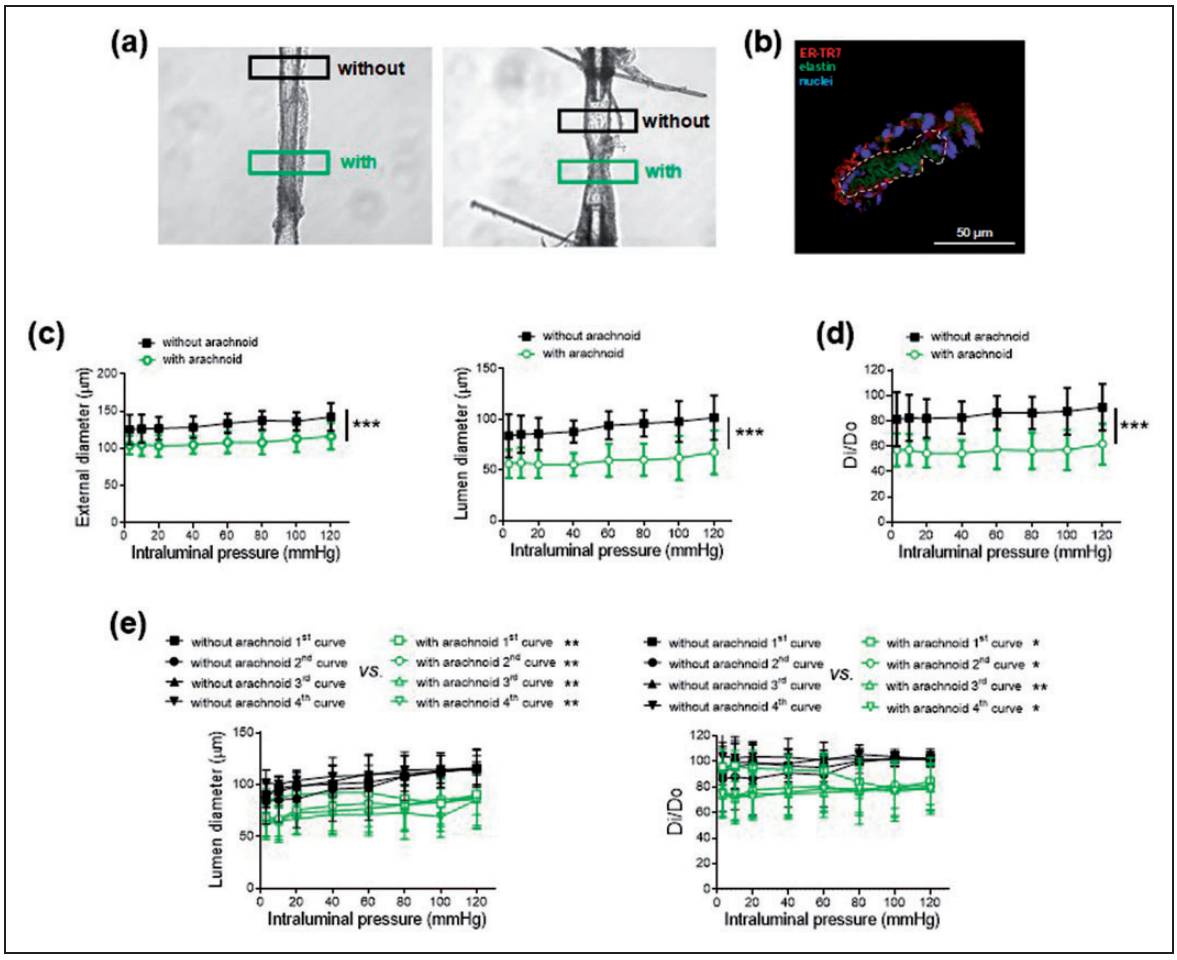

Figure 1. Effect of arachnoid tissue in Oncine France I mice middle cerebral arteries. (a) Representative images of two pressurized middle cerebral arteries with or without arachnoid tissue. Regions of interest are marked with a black (without arachnoid) and green (with arachnoid) rectangle. (b) Representative photomicrograph of the reticular fibroblast marker ER-TR7 immunofluorescence (red) of confocal microscopic mouse middle cerebral arteries ($n = 3$). Natural autofluorescence of elastin (green) and nuclear staining with Hoechst 33,342 (10 μg/ml) (blue) are also shown. The artery wall is marked with a dotted white line, and the surrounding outside tissue is arachnoid membrane. Effect of the absence (without) and presence (with) of arachnoid tissue on (c) external and lumen diameter-intraluminal pressure curves in active conditions (2.5 mM Ca^{2+}-Krebs-Henseleit solution) and (d) lumen diameter-intraluminal pressure curves in active (Di) relative to passive (D0) conditions (0 Ca^{2+}- Krebs-Henseleit solution) in male (55 %) and female (45 %) Oncine France I mice middle cerebral arteries. Results are the mean ± SD of 11 mice. ***$P < 0.001$ by 2-way ANOVA. (e) Effect of the absence (without) and presence (with) of arachnoid tissue on repetitive lumen diameter-intraluminal pressure curves (left) and lumen diameter-intraluminal pressure curves in Di relative to D0 conditions (right) in male Oncine France I mice middle cerebral arteries. Results are the mean ± SD of 5 mice. *$P < 0.05$, **$P < 0.01$ *vs.* without arachnoid by 2-way ANOVA.

Statistical analysis

Results are expressed as the mean ± SD of the number (n) of mice indicated in the figure legends. Normal distribution was checked when appropriate before choosing the statistical analysis. Comparison between two groups was carried out with the Mann-Whitney U or Student's t test. Comparison between more than two groups with two factors was carried out either with regular two-way ANOVA followed by Tukey's post-test or by two-way ANOVA with repeated measures on the concentration or intraluminal pressure factor. Mixed-effects model was used when comparisons were performed in the same artery. Data analysis was carried out using GraphPad Prism version 8.4.2 software (La Jolla, CA, USA). A value of $P \leq 0.05$ was considered significant.

Results

The arachnoid membrane increases the basal tone of the mouse MCA

Arachnoid membrane tissue was intentionally left in a region of the MCA and was compared to a contiguous (control) region without its presence (Figure 1(a) and

Supplementary Video). Positive staining for the reticular fibroblast marker ER-TR7 (Figure 1(b))[1] and negative staining for the neuron-specific marker βIII-tubulin confirmed that the tissue surrounding the MCA was actually the arachnoid membrane.

Both contractions to KCL (100 mM) and U46619 (1 nM–1 μM), and relaxations to SLIGRL (20 μM) were comparable between regions (Supplementary Figure 1(a)). Notably, when intraluminal pressure was increased stepwise in active conditions (2.5 mM Ca^{2+}-KHS), the region of the MCA with arachnoid tissue showed significantly lower external and lumen diameters compared to the region without this tissue (e.g. with arachnoid: 59.4 ± 15.9 μm *vs.* without arachnoid: 94.1 ± 13.9 μm, $n = 11$, 60 mmHg; $P < 0.001$) (Figure 1(c) and Supplementary Video). These differences were abolished when vessels were exposed to passive conditions (0 Ca^{2+}-KHS) (Supplementary Figure 2). In active conditions, slopes of the myogenic response-pressure curves (i.e. myogenic reactivity) showed no differences between regions (without arachnoid: 0.076 ± 0.14 *vs.* with arachnoid: 0.032 ± 0.12, $n = 11$). In contrast, lumen diameter reductions in active relative to passive conditions as a function of pressure were significantly larger in the region with arachnoid tissue (e.g. without arachnoid: $86.4 \pm 13.3\%$ *vs.* with arachnoid: 57.1 ± 14.9 %, $n = 11$, 60 mmHg; $P < 0.001$) (Figure 1(d)), suggesting an increase in basal (resting) tone. Basal tone values were comparable in regions with no arachnoid *vs.* vessels entirely cleaned of arachnoid (results not shown).

We then separated mice by sex and found that arachnoid tissue-dependent responses developed similarly in arteries of male and female mice (Supplementary Figure 3). We next explored the time-course of activation and maintenance of this response by exposing the MCA to four consecutive intraluminal pressure-diameter curves (Figure 1(e)). Both lumen diameter reductions and increased basal tones were observed at intraluminal pressures of 60–80 mmHg onwards during the first curve, and these differences were maintained throughout all curves tested. Overall, the results suggest that the arachnoid membrane increases the basal tone of the mouse MCA.

S1P is enriched in the arachnoid membrane

S1P lyase is present in the mouse arachnoid membrane[8] and S1P contracts murine cerebral arteries.[11,12] Raman imaging identified and allowed the marker-independent subcellular localization of S1P (Figure 2). A S1P Raman spectrum served as reference signature for TCA and resulted in intensity distribution heatmaps indicating a punctuate S1P distribution in all three layers of the mouse MCA wall (Figure 2(a)). Notably, a strong S1P signal was detected in arachnoid tissue, being localized primarily in the cytoplasm of reticular fibroblasts. Interestingly, the S1P Raman signal was also detected in a postmortem human MCA, showing a punctuate distribution along the endothelium and the media and adventitia layers of the artery. Notably, the most prominent S1P signal was observed in the reticular fibroblasts of the human arachnoid membrane (Figure 2(b)).

S1P mediates the arachnoid-induced basal tone increase

Exogenously added S1P contracted the MCA in a concentration-dependent manner regardless of the presence of arachnoid tissue (Figure 3(a)). This result indicates that the arachnoid membrane does not act as a diffusion hindrance to exogenously applied S1P under our "ex vivo" conditions. Previous studies demonstrated that S1P-induced contractions in the mouse and rat basilar artery are mostly mediated by $S1P_3R$.[11,12] The selective $S1P_3R$ antagonist TY 52156 (4 μM) dramatically reduced S1P-induced contractions in both regions (with and without arachnoid) (Figure 3 (a)). We then evaluated the influence of blocking $S1P_3R$ signaling on the arachnoid-induced effects. Incubation with TY 52156 partially prevented the arachnoid-induced lumen diameter decrease (Figure 3 (b)) and restored the basal tone increase (Figure 3(c)). Besides, inhibition of the ABCA1 S1P efflux transport with glibenclamide partially augmented the lumen diameter and prevented the basal tone increase in arachnoid regions (Supplementary Figure 4). Altogether, these data suggest that the vasoconstrictor effect on the MCA tone induced by the arachnoid membrane is mediated by S1P likely acting via $S1P_3R$.

Preserved arachnoid-induced responses during aging despite lower S1P levels

We next examined the influence of aging in the arachnoid-dependent responses. Quantitative analysis of Raman imaging showed a significant decrease in the arachnoid membrane-associated S1P signal during aging (Figure 4). As expected, the presence of arachnoid tissue in 3–4-month-old C57BL/6 wild-type mice caused a decrease in the lumen diameter (Supplementary Figure 5(a)) coupled with an increase in the basal tone (Figure 5(a)). In 8–9 month-old mice (middle age mice) compared to 3–4 month-old mice (young), the basal tone was significantly increased in regions without arachnoid tissue (without arachnoid 1st and 2nd curves; 8–9 month-old *vs.* 3–4 month-old; Supplementary Figure 6(a)). Notably, arachnoid regions of middle age mice still showed lower lumen

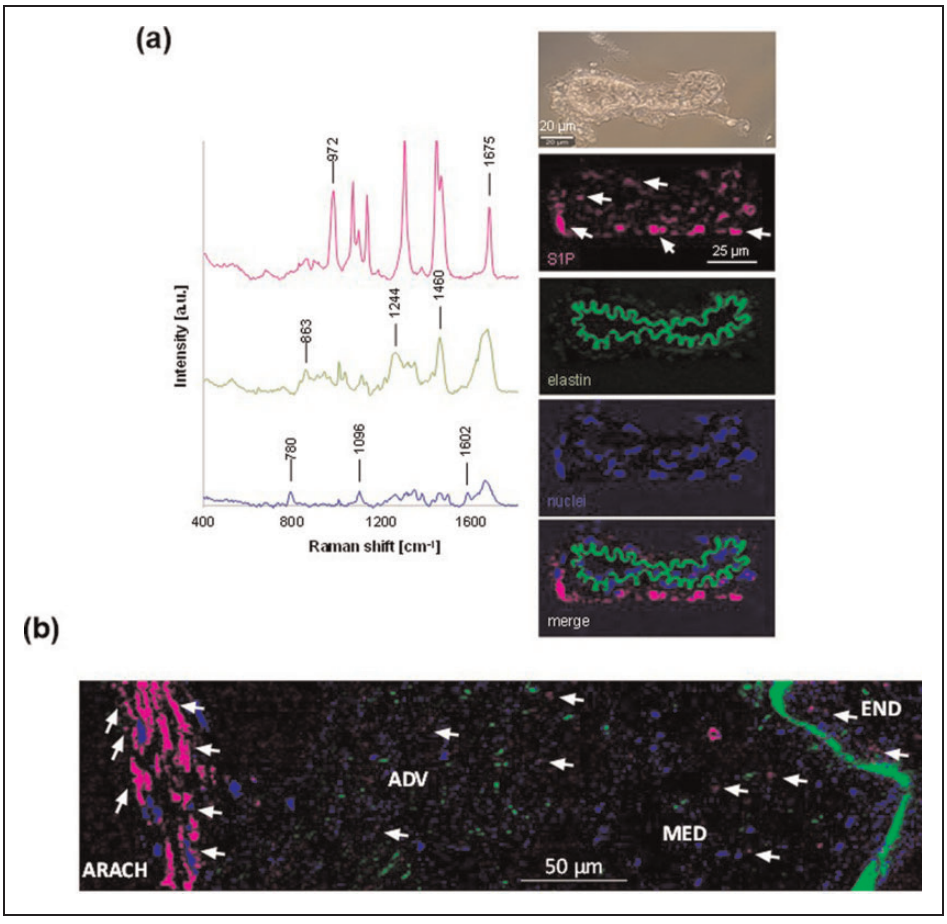

Figure 2. Raman imaging of sphingosine-1-phosphate (S1P) in middle cerebral arteries surrounded by arachnoid tissue. (a) Spectral signatures (left) identified by true component analysis assigned to S1P (pink), elastic fibers (green) and nuclei (blue), and (right) representative transmitted light image (above) and intensity distribution heatmaps (below) of microscopic male Oncine France 1 mice middle cerebral arteries ($n = 3$). Arrows point to positive S1P signal. (b) Representative intensity distribution heatmap of a microscopic male human middle cerebral artery. Arrows indicate examples of positive S1P signal. END, endothelium; MED, media; ADV, adventitia; ARACH, arachnoid.

diameters (with arachnoid 3rd and 4th curves; Supplementary Figure 5(a)) and higher basal tones (with arachnoid 3rd and 4th curves; Supplementary Figure 6(a); Figure 5(a)) than regions devoid of arachnoid, despite having lower arachnoid-associated S1P levels (Figure 4). Analysis of exogenous S1P (1 µM)-induced contractile responses showed higher vasoconstriction in 8-9-month-old mice (Figure 5(c)). These results suggest that arachnoid-induced increases in MCA tone are preserved in older mice because of a potential upregulation of S1PR signaling, which may compensate for the aging-associated reduced S1P levels in the arachnoid membrane.

Genetic deletion of SphK2 attenuates the arachnoid-induced increase in the basal tone

We subsequently studied the impact of SphK2 depletion in the arachnoid-associated effects on the MCA lumen diameter and basal tone. In arachnoid regions of 3–4-month-old SphK2$^{-/-}$ *vs.* wild-type mice, lumen diameters were slightly greater (Supplementary Figure 5) and basal tones were significantly decreased (e.g. with arachnoid 2nd curve; wild-type: 66.3 ± 9.8 %, SphK2$^{-/-}$: 84.6 ± 7.6 %, $n = 6$, 60 mmHg; Supplementary Figure 6). Importantly, in 3–4-months-old SphK2$^{-/-}$ mice, despite that the arachnoid membrane still produced a slight reduction in MCA lumen diameter (Supplementary Figure 5(b)), the effect on the basal tone was absent (Supplementary Figure 6(b); Figure 5(b)). In addition, MCA from 8–9-month-old SphK2$^{-/-}$ mice showed marginal arachnoid-induced responses (Supplementary Figure 5(b); Supplementary Figure 6(b); Figure 5(b)). Besides, contractile responses to exogenous S1P (1 µM) were similar in SphK2$^{-/-}$ *vs.* 3-4-months-old wild-type mice, whereas the increased S1PR signaling observed in 8–9-months-old wild-type mice was normalized in SphK2$^{-/-}$ mice (Figure 5(c)). The unaltered exogenous S1P responses in

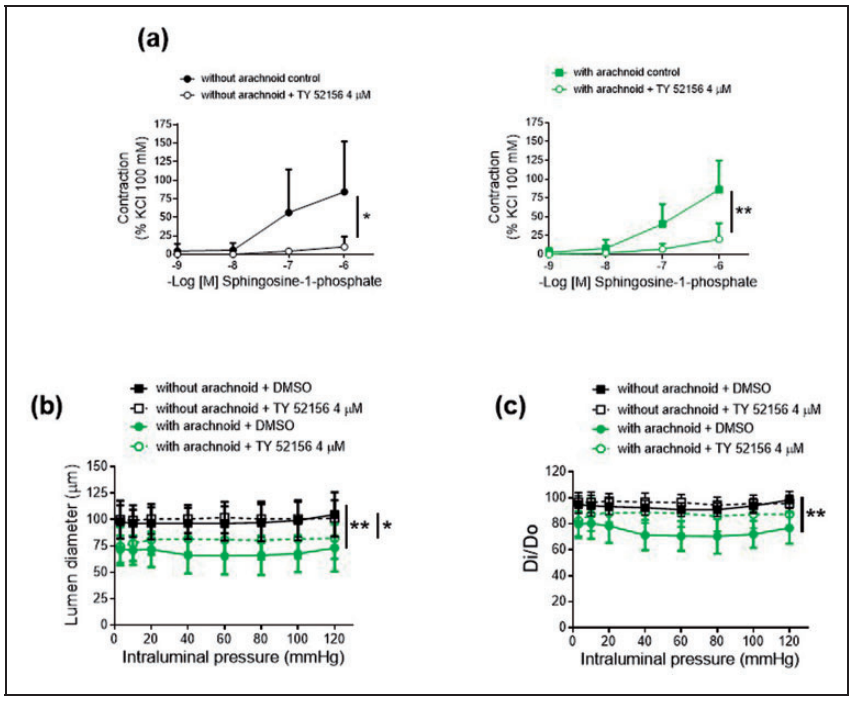

Figure 3. Characterization of sphingosine-1-phosphate responses in male Oncine France 1 mice middle cerebral arteries. (a) Concentration-response curves to sphingosine-1-phosphate. Results are the mean ± SD of 5 mice. $*P < 0.05$, $**P < 0.01$ by 2-way ANOVA. Effect of the absence (without) and presence (with) of arachnoid tissue on (b) lumen diameter-intraluminal pressure curves in active conditions (2.5 mM Ca^{2+}-Krebs-Henseleit solution) and (c) lumen diameter-intraluminal pressure curves in active (Di) relative to passive (D0) conditions (0 Ca^{2+}-Krebs-Henseleit solution) in the absence and presence of TY 52156 (4 μM). Results are the mean ± SD of 6 mice. $*P < 0.05$, $**P < 0.01$ by 2-way ANOVA.

$SphK2^{-/-}$ mice suggests that attenuation of arachnoid-induced vasoconstriction could be attributed to a process upstream S1PR signaling. Consistently, quantitative Raman imaging showed a significant reduction of the arachnoid membrane-associated S1P signal in $SphK2^{-/-}$ mice (Figure 6).

Discussion

Perivascular tissue can influence vascular tone by releasing vasoactive factors able to modulate VSMC contractility. The present study reveals a functional coupling between the arachnoid membrane and the MCA that promotes tonic vasoconstriction, and suggests a key role for S1P as the factor that mediates this crosstalk via $S1P_3R$ signaling. Moreover, we show that, in spite of the aging-related reduction of S1P levels, arachnoid-induced responses still occur. Finally, we show that SphK2 is central for the arachnoid-derived vasoconstrictor stimuli.

The arachnoid membrane regulates MCA tone

Typically, adjacent vascular tissues were considered a structural component of the blood vessels. However, increasing evidence that perivascular tissue is essential to modulate vessel function in health and disease has focused attention on the "outside to inside" crosstalk paradigm between surrounding tissue and blood vessels.[32,33] Cerebral vessels that run on the brain surface are in tight contact with the arachnoid and pia membranes, which are separated by a CSF-filled space. Our results show that arachnoid tissue exerts a significant tonic vasoconstriction on the mouse MCA basal tone, whereas it does not influence myogenic reactivity or the agonist-induced responses tested. This finding is striking, because it demonstrates that the arachnoid membrane is more than just a structure that delimits the subarachnoid compartment, as it actively influences cerebral artery tone and likely contributes to adjust local cerebral blood flow. Recent studies have proposed the presence of directed fluid flow in the paravascular space surrounding cerebral arteries mainly because of heart beat pulsations.[34–40] We speculate that the arachnoid-induced vasoconstriction may play a role in modulating CSF flow, since it produces a significant influence on the MCA lumen diameter. This homeostatic mechanism may aid metabolic waste products clearance and maintenance of the ionic environment in the brain.[41,42]

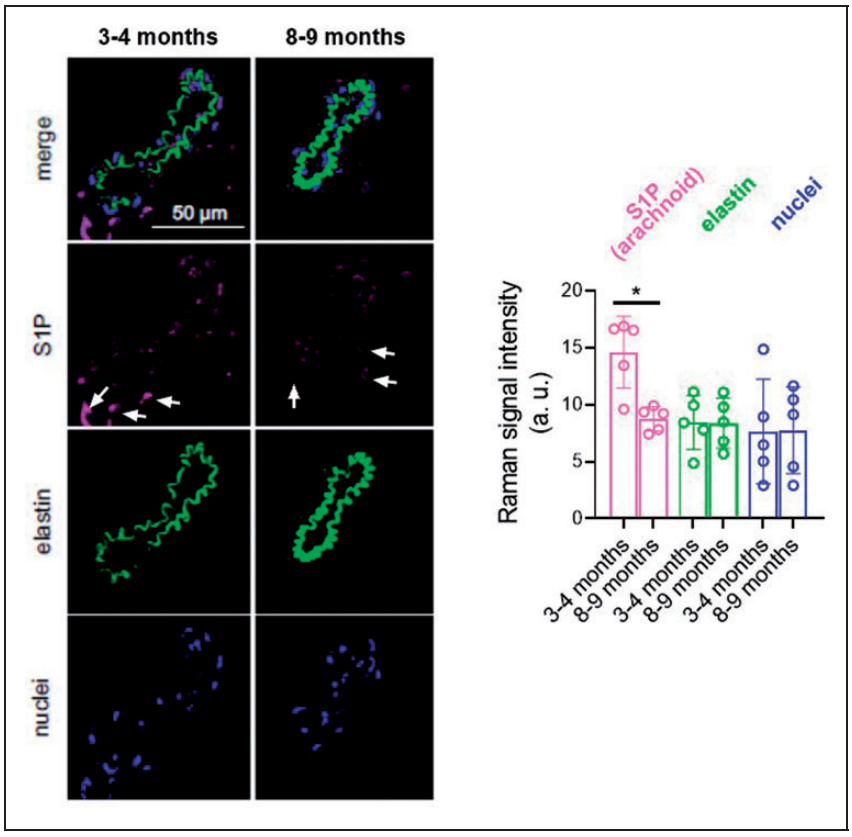

Figure 4. Quantitative Raman imaging of sphingosine-1-phosphate (S1P) in arachnoid tissue surrounding C57BL/6 mice middle cerebral arteries. Representative intensity distribution heatmaps and quantitative analysis of microscopic 3- to 4-month-old (60% male/40% female) and 8- to 9-month-old (60% male/40% female) mice middle cerebral arteries identified by true component Raman analysis assigned to S1P (pink), elastic fibers (green) and nuclei (blue). Arrows indicate examples of positive S1P signal. Results are the mean ± SD of 5 mice. $^{*}P < 0.05$ by Mann-Whitney U test.

S1P arbitrates the arachnoid-induced vasoconstriction: receptor signaling and influence of aging

Endothelial cells serve as a reservoir of S1P in the vascular wall.[43] The discovery that S1P lyase is expressed in the murine arachnoid mater[8] suggests that S1P released from the arachnoid membrane could be a potential candidate to mediate the observed arachnoid-dependent vasoconstriction. Actually, we show that the arachnoid membrane is enriched in S1P, displaying greater amounts than those in the MCA wall. Notice that the arachnoid is a translucent membrane that is composed of tightly packed epithelial cells that form a barrier and a central layer composed of fibroblast-like cells and collagenous trabeculae. Although we cannot exclude the presence of S1P in epithelial cells, Raman results shown here suggest that fibroblast-like cells are the main source of S1P in both mice and humans.

In the brain, S1P signaling plays an important role in cerebral artery vasoconstriction by acting either extracellularly on $S1P_3R$[11,12] or intracellularly in response to vasoconstrictors.[17] In addition, S1P has been involved in the regulation of cerebral myogenic responsiveness in mouse olfactory cerebral arteries in the context of subarachnoid hemorrhage.[44] Our results point to S1P as the mediator responsible for the arachnoid-induced vasoconstrictor effects in the mouse MCA, because: i) the strongest positive signal for S1P is detected in arachnoid tissue surrounding the MCA from mice (OF1 and C57BL/6 strains) and the human specimen; ii) the ABCA1 transporter inhibitor glibenclamide, which partially blocks S1P release from human vascular endothelial cells,[28] inhibits the arachnoid-derived vasoconstrictor effects on the MCA tone; iii) $S1P_3R$ antagonism with TY 52156 prevents both exogenous S1P-induced contractile responses and the arachnoid-dependent increase in the basal tone; and iv) genetic deletion of SphK2 reduces arachnoid S1P content and vasoconstriction.

The vasoconstrictor influence of S1P on MCA tone persisted over time, suggesting a continuous production of S1P by SphK and/or sufficient amounts of preformed S1P. The stimulus that may release S1P from

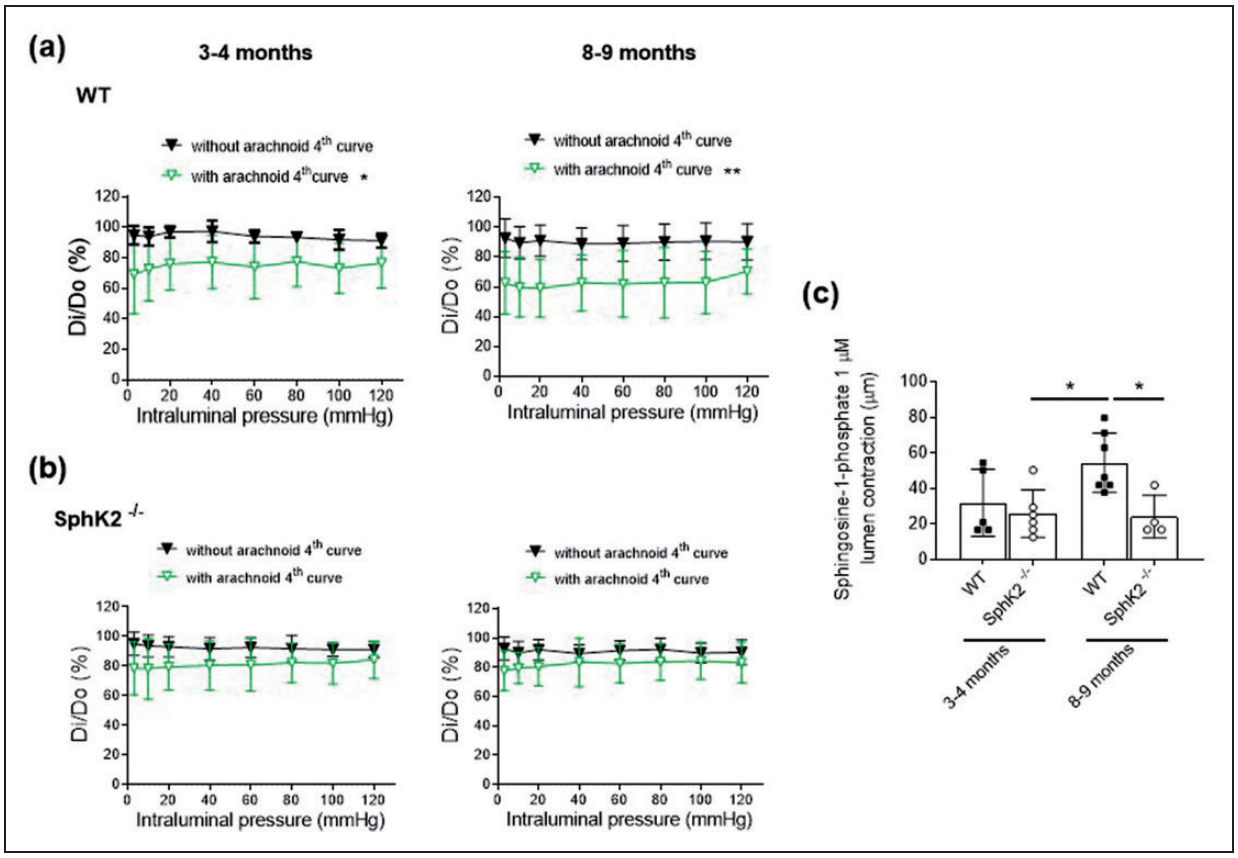

Figure 5. Influence of aging and genetic deletion of sphingosine kinase 2 (SphK2$^{-/-}$) on middle cerebral artery responses in C57BL/6 mice. (a) Effect of the absence (without) and presence (with) of arachnoid tissue on the 4th lumen diameter-intraluminal pressure curve in active (Di) relative to passive (D0) conditions (0 Ca^{2+}-Krebs-Henseleit solution) in 3- to 4-month-old (67% male/33% female) and 8- to 9-month-old (50% male/50% female) wild-type (WT) mice. Results are the mean ± SD of 6-8 mice. *$P < 0.05$, **$P < 0.01$ *vs.* by 2-way ANOVA. (b) Effect of the absence (without) and presence (with) of arachnoid tissue on the 4th lumen diameter-intraluminal pressure curve in Di relative to D0 conditions in 3- to 4-month-old (33% male/67% female) and 8- to 9-month-old (50% male/50% female) SphK2$^{-/-}$ mice. Results are the mean ± SD of 6 mice. (c) Lumen contraction to 1 µM sphingosine-1-phosphate (S1P) in middle cerebral arteries without arachnoid tissue. Results are the mean ± SD of 4-7 mice. *$P < 0.05$ by 2-way ANOVA.

the arachnoid membrane to regulate MCA tone is unknown. Previous studies suggest that laminar shear stress induces the discharge of S1P from endothelial cells.[45] Moreover, mechanical stretch on VSMCs in response to increased transmural pressure activates endogenous S1P signaling leading to myogenic vasoconstriction.[18,46] Nevertheless, how transmural pressure orchestrates the signaling cascades in arachnoid cells stimulating the release of S1P remains an open question. On the other hand, our results suggest that $S1P_3R$ signaling governs S1P-induced responses in the mouse MCA in agreement with previous studies in the rat and mouse basilar artery.[11,12] In addition, $S1P_3R$ signaling mediates vasoconstriction in response to either exogenous S1P or increments in intraluminal pressure in mouse mesenteric arteries,[47] as well as in rat coronary and canine cerebral artery contractions.[27] Besides, $S1P_2R$ signaling influences regional blood flow and vascular resistance in the renal and mesenteric territory of mice[48] and participates in the constriction of hamster gracilis muscle arteries.[46] Altogether, these studies suggest that differences in S1PR signaling exist between arterial beds and/or species.

S1P signaling increases mouse olfactory cerebral artery tone following subarachnoid hemorrhage and S1PR antagonism treatment is beneficial[44] In addition, a recent study reported higher S1P levels in the CSF of patients with subarachnoid hemorrhage.[49] We suggest that arachnoid S1P could have an active role in the disease process after subarachnoid hemorrhage, for instance, by contributing to vasospasm, which has been associated with poor outcomes.[50] Moreover, potentially differential arachnoid-dependent responses along the main trunk, the pial territory and the proximal and peripheral regions of the MCA may have a crucial impact in vasospasm and/or delayed cerebral

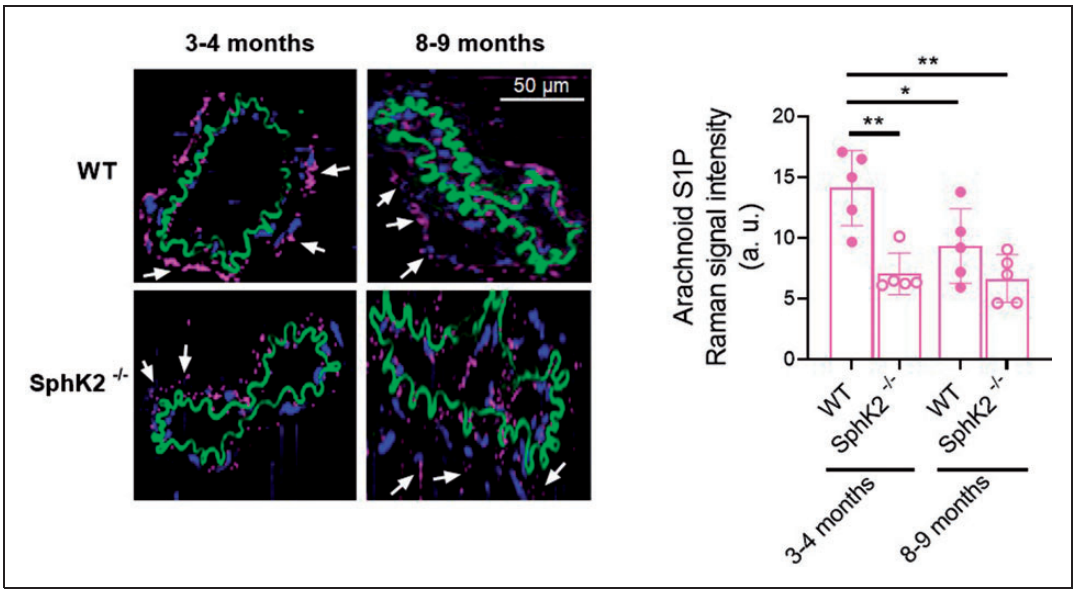

Figure 6. Quantitative Raman imaging of sphingosine-1-phosphate (S1P) in arachnoid tissue surrounding sphingosine kinase 2 knockout (SphK2$^{-/-}$) and wild-type (WT) mice middle cerebral arteries. Representative intensity distribution heatmaps (left) and quantitative analysis (right) of microscopic 3- to 4-month-old (50% male/50% female) and 8- to 9-month-old (60% male/40% female) mice middle cerebral arteries identified by true component analysis assigned to S1P (pink). Elastic fibers (green) and nuclei (blue) are also shown. Arrows point to S1P signal in arachnoid tissue. Results are represented as mean Raman signal intensities ± SD of 5 mice. *$P < 0.05$, **$P < 0.01$ by 2-way ANOVA.

ischemia after subarachnoid hemorrhage. Notably, evidence on the impact of aging in S1P signaling is scarce. Couttas et al. reported an age-dependent marked decline in the S1P/sphingosine ratio in the hippocampus of female subjects over 65 years.[51] Here, the arachnoid-induced effects persisted in middle age mice in spite of the reduction of arachnoid S1P deposits compared to young mice, suggesting that the arachnoid-induced modulation of myogenic tone could be a tightly controlled mechanism to regulate cerebral blood flow during aging. We hypothesize that this effect could be associated with an improved smooth muscle S1PR signaling, since exogenous S1P induced higher contractions in older animals. Previous studies have reported decreased pulsatility of the MCA in Alzheimer's disease patients,[52] which could develop into a failure of CSF-dependent drainage of amyloid-beta peptides.[53,54] We speculate that a decrease of arachnoid S1P deposits with age could finally impair arachnoid-induced vasoconstriction, resulting in reduced vessel wall pulsatility and impaired drainage of amyloid-beta peptides to the CSF.

SphK2 is a main effector of the arachnoid-induced vasoconstrictor stimuli

A functional redundancy for viability exists between SphK1 and SphK2, because a single isoform deletion has no major effect on the phenotype, whereas double deletion is lethal due to defective vascular development.[55] However, some significant phenotypic differences occur between mice with SphK isoform-specific deletion, which suggests that these enzymes have different physiological roles depending on the context.[4] Differential effects of both enzymes may depend on their cellular and tissue localization, which could determine the inside-out signaling of S1P in response to extracellular stimuli.[4] For instance, SphK1 is generally located in the cytosol and can be translocated across the plasma membrane, whereas SphK2 is mainly detected in the nucleus, endoplasmic reticulum and mitochondria.[56] In the present study, arachnoid S1P signal in fibroblasts-like cells shows a cytoplasmic distribution, which does not exclude the participation of either isoform of SphK in S1P synthesis. Although SphK2 is the predominant isoform in brain parenchyma,[19,57] both isoforms are expressed in cerebral arteries.[17] We found that SphK2 genetic deficiency reduced arachnoid S1P levels, attenuated arachnoid-induced vasoconstriction and normalized the increased S1PR signaling in middle age mice. However, the arachnoid-induced vasoconstrictor effect still slightly developed after SphK2 depletion, suggesting the potential contribution of a SphK1-dependent S1P pool in this response. This is not surprising, since SphK1 is a major determinant of resting tone in resistance arteries.[13–16] Furthermore, in the brain, SphK1 modulates vasoconstriction in the rat basilar artery[17] and

participates in rabbit posterior cerebral artery myogenic tone.[18]

Study limitations

We identify some limitations of the present work. First, although pressure myography is the gold standard for measuring blood vessel function "ex vivo", we cannot exclude the possibility of differences "in vivo" due to a plausible contribution of CSF to the cross talk between the arachnoid membrane and the MCA. The presence of such great amounts of S1P in the arachnoid membrane likely guarantees a biologically relevant function of this bioactive lipid in this tissue. Second, the arachnoid-induced effects may not happen in all cerebral arteries. We attempted reproducing the same experiment in basilar arteries, though we were not able to retain arachnoid tissue consistently in this vascular bed. Nevertheless, arachnoid fibroblasts are present around arteries and veins in the meninges, as well as around penetrating arterioles and venules,[1] which suggests that S1P might be widely distributed around brain vessels.

Conclusions

For the first time, the arachnoid membrane is identified as an important source of S1P. We suggest that this lipid mediates arachnoid-induced modulation of MCA tone through $S1P_3R$ signaling. Altogether, these data establish a new paradigm for the S1P actions on the cerebral vasculature and could provide a novel target to modulate cerebral blood flow in disease.

Funding

The author(s) disclosed receipt of the following financial support for the research, authorship, and/or publication of this article: This work was supported by *Fundació La Marató de TV3* [201716-10]; the *Ministerio de Ciencia e Innovación* [SAF2014-56111-R, SAF2017-83039-R and SAF2017-87459-R]; the *Generalitat de Catalunya* [SGR-645]; the *Ministry of Science, Research and the Arts of Baden-Württemberg* [33-729.55-3/214 and SI-BW 01222-91]; and the *Deutsche Forschungsgemeinschaft* [INST 2388/64-1 and GRK 2543/1].

Acknowledgements

We thank the Microscopy Unit of *Serveis Científico-Tècnics* of the Autonomous University of Barcelona for technical support.

Declaration of conflicting interests

The author(s) declared no potential conflicts of interest with respect to the research, authorship, and/or publication of this article.

Authors' contributions

FJ-A made a substantial contribution to the concept and design and drafted the article. FJ-A, JM, MG, APD, MO and SR made a substantial contribution to the acquisition of data or analysis and interpretation of data. FJ-A, JM, MG, APD, MO, SR, GE, KS-L, EJ-X and AP revised the manuscript critically for important intellectual content, and approved the version to be published. Data will be provided upon request.

Supplemental material

Supplemental material for this article is available online.

ORCID iDs

Francesc Jiménez-Altayó https://orcid.org/0000-0002-9034-2041
Julia Marzi https://orcid.org/0000-0003-1545-5430
Anna M Planas https://orcid.org/0000-0002-6147-1880

References

1. Hannocks MJ, Pizzo ME, Huppert J, et al. Molecular characterization of perivascular drainage pathways in the murine brain. *J Cereb Blood Flow Metab* 2018; 38: 669–686.
2. Mastorakos P and McGavern D. The anatomy and immunology of vasculature in the central nervous system. *Sci Immunol* 2019; 4: eaav0492.
3. Bjorefeldt A, Illes S, Zetterberg H, et al. Neuromodulation via the cerebrospinal fluid: insights from recent in vitro studies. *Front Neural Circuits* 2018; 12: 5.
4. Strub GM, Maceyka M, Hait NC, et al. Extracellular and intracellular actions of sphingosine-1-phosphate. *Adv Exp Med Biol* 2010; 688: 141–155.
5. Kim RH, Takabe K, Milstien S, et al. Export and functions of sphingosine-1-phosphate. *Biochim Biophys Acta* 2009; 1791: 692–696.
6. Wang Z, Zheng Y, Wang F, et al. Mfsd2a and Spns2 are essential for sphingosine-1-phosphate transport in the formation and maintenance of the blood-brain barrier. *Sci Adv* 2020; 6: eaay8627.
7. Pyne S, Adams DR and Pyne NJ. Sphingosine 1-phosphate and sphingosine kinases in health and disease: recent advances. *Prog Lipid Res* 2016; 62: 93–106.
8. Borowsky AD, Bandhuvula P, Kumar A, et al. Sphingosine-1-phosphate lyase expression in embryonic and adult murine tissues. *J Lipid Res* 2012; 53: 1920–1931.
9. Mendelson K, Evans T and Hla T. Sphingosine 1-phosphate signalling. *Development* 2014; 141: 5–9.
10. Sasset L, Zhang Y, Dunn TM, et al. Sphingolipid de novo biosynthesis: a rheostat of cardiovascular homeostasis. *Trends Endocrinol Metab* 2016; 27: 807–819.
11. Salomone S, Yoshimura S, Reuter U, et al. S1P3 receptors mediate the potent constriction of cerebral arteries by sphingosine-1-phosphate. *Eur J Pharmacol* 2003; 469: 125–134.

12. Salomone S, Potts EM, Tyndall S, et al. Analysis of sphingosine 1-phosphate receptors involved in constriction of isolated cerebral arteries with receptor null mice and pharmacological tools. *Br J Pharmacol* 2008; 153: 140–147.
13. Bolz SS, Vogel L, Sollinger D, et al. Sphingosine kinase modulates microvascular tone and myogenic responses through activation of RhoA/rho kinase. *Circulation* 2003; 108: 342–347.
14. Lidington D, Peter BF, Meissner A, et al. The phosphorylation motif at serine 225 governs the localization and function of sphingosine kinase 1 in resistance arteries. *Arterioscler Thromb Vasc Biol* 2009; 29: 1916–1922.
15. Keller M, Lidington D, Vogel L, et al. Sphingosine kinase functionally links elevated transmural pressure and increased reactive oxygen species formation in resistance arteries. *Faseb J* 2006; 20: 702–704.
16. Yang J, Noyan-Ashraf MH, Meissner A, et al. Proximal cerebral arteries develop myogenic responsiveness in heart failure via tumor necrosis factor-alpha-dependent activation of sphingosine-1-phosphate signaling. *Circulation* 2012; 126: 196–206.
17. Salomone S, Soydan G, Ip PC, et al. Vessel-specific role of sphingosine kinase 1 in the vasoconstriction of isolated basilar arteries. *Pharmacol Res* 2010; 62: 465–474.
18. Lim M, Choi SK, Cho YE, et al. The role of sphingosine kinase 1/sphingosine-1-phosphate pathway in the myogenic tone of posterior cerebral arteries. *PLoS One* 2012; 7: e35177.
19. Pfeilschifter W, Czech-Zechmeister B, Sujak M, et al. Activation of sphingosine kinase 2 is an endogenous protective mechanism in cerebral ischemia. *Biochem Biophys Res Commun* 2011; 413: 212–217.
20. Wacker BK, Park TS and Gidday JM. Hypoxic preconditioning-induced cerebral ischemic tolerance: role of microvascular sphingosine kinase 2. *Stroke* 2009; 40: 3342–3348.
21. Yung LM, Wei Y, Qin T, et al. Sphingosine kinase 2 mediates cerebral preconditioning and protects the mouse brain against ischemic injury. *Stroke* 2012; 43: 199–204.
22. Wacker BK, Freie AB, Perfater JL, et al. Junctional protein regulation by sphingosine kinase 2 contributes to blood-brain barrier protection in hypoxic preconditioning-induced cerebral ischemic tolerance. *J Cereb Blood Flow Metab* 2012; 32: 1014–1023.
23. Jiménez-Altayó F, Caracuel L, Pérez-Asensio FJ, et al. Participation of oxidative stress on rat middle cerebral artery changes induced by focal cerebral ischemia: beneficial effects of 3,4-dihydro-6-hydroxy-7-methoxy-2,2-dimethyl-1(2H)-benzopyran (CR-6). *J Pharmacol Exp Ther* 2009; 331: 429–436.
24. Cipolla MJ, Lessov N, Hammer ES, et al. Threshold duration of ischemia for myogenic tone in middle cerebral arteries: effect on vascular smooth muscle actin. *Stroke* 2001; 32: 1658–1664.
25. Onetti Y, Dantas AP, Pérez B, et al. Middle cerebral artery remodeling following transient brain ischemia is linked to early postischemic hyperemia: a target of uric acid treatment. *Am J Physiol Heart Circ Physiol* 2015; 308: H862–874.
26. Dantas AP, Onetti Y, Oliveira MA, et al. Western diet consumption promotes vascular remodeling in non-senescent mice consistent with accelerated senescence, but does not modify vascular morphology in senescent ones. *Exp Gerontol* 2014; 55: 1–11.
27. Murakami A, Takasugi H, Ohnuma S, et al. Sphingosine 1-phosphate (S1P) regulates vascular contraction via S1P3 receptor: investigation based on a new S1P3 receptor antagonist. *Mol Pharmacol* 2010; 77: 704–713.
28. Lee Y-M, Venkataraman K, Hwang S-I, et al. A novel method to quantify sphingosine 1-phosphate by immobilized metal affinity chromatography (IMAC). *Prostaglandins Other Lipid Mediat* 2007; 84: 154–162.
29. Zbinden A, Marzi J, Schlünder K, et al. Non-invasive marker-independent high content analysis of a microphysiological human pancreas-on-a-chip model. *Matrix Biol* 2020; 85-86: 205–220.
30. Marzi J, Biermann AC, Brauchle EM, et al. Marker-independent in situ quantitative assessment of residual cryoprotectants in cardiac tissues. *Anal Chem* 2019; 91: 2266–2272.
31. Spiers RM, Marzi J, Brauchle EM, et al. Donor age significantly influences the Raman spectroscopic biomolecular fingerprint of human pancreatic extracellular matrix proteins following collagenase-based digestion. *Acta Biomater* 2019; 99: 269–283.
32. Aalbaek F, Bonde L, Kim S, et al. Perivascular tissue inhibits rho-kinase-dependent smooth muscle Ca(2+) sensitivity and endothelium-dependent H2S signalling in rat coronary arteries. *J Physiol* 2015; 593: 4747–4764.
33. Fernández-Alfonso MS, Somoza B, Tsvetkov D, et al. Role of perivascular adipose tissue in health and disease. *Compr Physiol* 2017; 8: 23–59.
34. Iliff JJ, Wang M, Zeppenfeld DM, et al. Cerebral arterial pulsation drives paravascular CSF–interstitial fluid exchange in the murine brain. *J Neurosci* 2013; 33: 18190–18199.
35. Bedussi B, Almasian M, de Vos J, et al. Paravascular spaces at the brain surface: low resistance pathways for cerebrospinal fluid flow. *J Cereb Blood Flow Metab* 2018; 38: 719–726.
36. Mestre H, Tithof J, Du T, et al. Flow of cerebrospinal fluid is driven by arterial pulsations and is reduced in hypertension. *Nat Commun* 2018; 9: 4878.
37. Bilston LE, Fletcher DF, Brodbelt AR, et al. Arterial pulsation-driven cerebrospinal fluid flow in the perivascular space: a computational model. *Comput Methods Biomech Biomed Engin* 2003; 6: 235–241.
38. Schley D, Carare-Nnadi R, Please CP, et al. Mechanisms to explain the reverse perivascular transport of solutes out of the brain. *J Theor Biol* 2006; 238: 962–974.
39. Wang P and Olbricht WL. Fluid mechanics in the perivascular space. *J Theor Biol* 2011; 274: 52–57.
40. Kedarasetti RT, Turner KL, Echagarruga C, et al. Functional hyperemia drives fluid exchange in the paravascular space. *Fluids Barriers CNS* 2020; 17: 52.
41. Iliff JJ, Wang M, Liao Y, et al. A paravascular pathway facilitates CSF flow through the brain parenchyma and

the clearance of interstitial solutes, including amyloid beta. *Sci Transl Med* 2012; 4: 147ra111.
42. Abbott NJ, Pizzo ME, Preston JE, et al. The role of brain barriers in fluid movement in the CNS: is there a 'glymphatic' system? *Acta Neuropathol* 2018; 135: 387–321.
43. Ancellin N, Colmont C, Su J, et al. Extracellular export of sphingosine kinase-1 enzyme. Sphingosine 1-phosphate generation and the induction of angiogenic vascular maturation. *J Biol Chem* 2002; 277: 6667–6675.
44. Yagi K, Lidington D, Wan H, et al. Therapeutically targeting tumor necrosis factor-α/sphingosine-1-Phosphate signaling corrects myogenic reactivity in subarachnoid hemorrhage. *Stroke* 2015; 46: 2260–2270.
45. Venkataraman K, Lee YM, Michaud J, et al. Vascular endothelium as a contributor of plasma sphingosine 1-phosphate. *Circ Res* 2008; 102: 669–676.
46. Peter BF, Lidington D, Harada A, et al. Role of sphingosine-1-phosphate phosphohydrolase 1 in the regulation of resistance artery tone. *Circ Res* 2008; 103: 315–324.
47. Cantalupo A, Gargiulo A, Dautaj E, et al. S1PR1 (sphingosine-1-Phosphate receptor 1) signaling regulates blood flow and pressure. *Hypertension* 2017; 70: 426–434.
48. Lorenz JN, Arend LJ, Robitz R, et al. Vascular dysfunction in S1P2 sphingosine 1-phosphate receptor knockout mice. *Am J Physiol Regul Integr Comp Physiol* 2007; 292: R440–446.
49. Männer A, Thomas D, Wagner M, et al. Sphingosine 1-phosphate levels in cerebrospinal fluid after subarachnoid hemorrhage. *Neurol Res Pract* 2020; 2: 49.
50. Macdonald RL, Pluta RM and Zhang JH. Cerebral vasospasm after subarachnoid hemorrhage: the emerging revolution. *Nat Clin Pract Neurol* 2007; 3: 256–263.
51. Couttas TA, Kain N, Tran C, et al. Age-dependent changes to sphingolipid balance in the human hippocampus are gender-specific and may sensitize to neurodegeneration. *J Alzheimers Dis* 2018; 63: 503–514.
52. Ortner M, Hauser C, Schmaderer C, et al. Decreased vascular pulsatility in Alzheimer's disease dementia measured by transcranial color-coded duplex sonography. *Neuropsychiatr Dis Treat* 2019; 15: 3487–3499.
53. Weller RO, Subash M, Preston SD, et al. Perivascular drainage of amyloid-beta peptides from the brain and its failure in cerebral amyloid angiopathy and Alzheimer's disease. *Brain Pathol* 2008; 18: 253–266.
54. Kwon S, Moreno-Gonzalez I, Taylor-Presse K, et al. Impaired peripheral lymphatic function and cerebrospinal fluid outflow in a mouse model of Alzheimer's disease. *J Alzheimers Dis* 2019; 69: 585–593.
55. Mizugishi K, Yamashita T, Olivera A, et al. Essential role for sphingosine kinases in neural and vascular development. *Mol Cell Biol* 2005; 25: 11113–11121.
56. Sanllehí P, Abad JL, Casas J, et al. Inhibitors of sphingosine-1-phosphate metabolism (sphingosine kinases and sphingosine-1-phosphate lyase). *Chem Phys Lipids* 2016; 197: 69–81.
57. Blondeau N, Lai Y, Tyndall S, et al. Distribution of sphingosine kinase activity and mRNA in rodent brain. *J Neurochem* 2007; 103: 509–517.